HHS Public Access

Author manuscript

ChemMedChem. Author manuscript; available in PMC 2018 December 19.

Published in final edited form as:

ChemMedChem. 2017 December 19; 12(24): 2030–2043. doi:10.1002/cmdc.201700449.

Design, Synthesis, Molecular Modeling, and Biological Evaluation of Novel Amine-based Histone Deacetylase Inhibitors

Dr. Hazem Abdelkarim[†], **Dr. Raghupathi Neelarapu**[†], **Antonett Madriaga**[†], **Dr. Aditya S. Vaidya**[†], **Dr. Irida Kastrati**[‡], **Dr. Yue-ting Wang**[†], **Taha Y. Taha**[†], **Prof. Gregory R. J. Thatcher**[†], **Prof. Jonna Frasor**[‡], and **Prof. Pavel A. Petukhov**[†,*]

[†]Department of Medicinal Chemistry and Pharmacognosy, College of Pharmacy, University of Illinois at Chicago, 833 South Wood Street, Chicago, IL 60612, USA

[‡]Department of Physiology and Biophysics, University of Illinois at Chicago, Chicago, IL 60612, USA

Abstract

Histone deacetylases (HDACs) are promising drug targets for a variety of therapeutic applications. Here we describe the design, synthesis, biological evaluation in cellular models of cancer, and preliminary drug metabolism and pharmacokinetic studies (DMPK) of a series of secondary and tertiary N-substituted 7-aminoheptanoic acid hydroxyamide-based HDAC inhibitors **2** and **3**, respectively. Introduction of an amino group with one or two surface binding groups (SBGs) yielded a successful strategy to develop novel and potent HDAC inhibitors. Secondary amines **2** were found to be generally more potent than the corresponding tertiary amines **3**. Docking studies suggested that the SBGs of tertiary amines **3** cannot be favorably accommodated at the gorge region of the binding site. The secondary amines with naphthalen-2-ylmethyl (**2g**), 1H-indol-2-ylmethyl (**2j**), and 5-phenylthiophen-2-ylmethyl (**2l**) substituents exhibited the highest potency against class I HDACs: HDAC1 IC_{50} 39–61 nM, HDAC2 IC_{50} 260–690 nM, HDAC3 IC_{50} 25–68 nM, and HDAC8 IC_{50} 320–620 nM. The cytotoxicity of a representative set of secondary and tertiary N-substituted 7-aminoheptanoic acid hydroxyamide-based inhibitors against HT-29, SH-SY5Y, and MCF-7 cancer cells correlated with their inhibition of HDAC1, 2, and 3 and was comparable to or better than that of SAHA (**1**). Compounds in this series increased acetylation of histones H3 and H4 in a time-dependent manner. DMPK studies indicated that secondary amine **2j** is metabolically stable and has plasma and brain concentrations >23- and >1.6-fold higher than the IC_{50} for class I HDACs, respectively. Overall, the secondary and tertiary N-substituted 7-aminoheptanoic acid hydroxyamide-based inhibitors exhibit excellent leadlike/druglike properties and therapeutic capacity for cancer applications.

Graphical abstract

[*]Corresponding author: Phone: 312-996-4174. Fax: 312-996-7107. pap4@uic.edu.

Supporting Information **Available:** Synthetic and analytical methods for the compounds described herein; detailed description of the activity assay, photolabeling experiments, molecular analysis, and docking calculations; Supplementary Figures S1–S4 and Tables S1–S2.

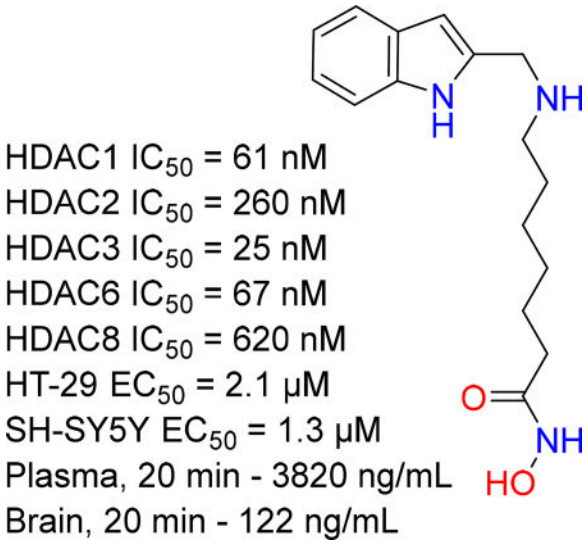

Keywords

Antitumor agents; Histone deacetylase; Inhibitors; Amines; Epigenetics

Introduction

Histone deacetylases (HDACs) are key epigenetic regulators.[1] The zinc-dependent HDACs are divided into three classes based on structure, sequence homology, and domain organization.[1] Class I consists of HDACs 1, 2, 3, and 8, class II – HDACs 4, 5, 6, 7, 9, and 10, and class IV – HDAC 11. Deacetylation of histone substrates results in an overall change in the post-translational state of histones, known as the “histone code”.[2] The list of cellular events controlled by HDACs has grown beyond DNA replication, DNA repair, chromatin remodeling, and gene transcription to non-histone targets and noncoding mRNA, and it continues to expand.[3] Normal regulation of these processes is compromised in a variety of diseases and conditions, and altered HDAC expression/function has been shown to be a hallmark of many cancers and neurodegenerative and inflammatory diseases.[3b, 4] Because of the roles HDACs play in these diseases, they have emerged as potential therapeutic targets. The FDA has approved pan-HDAC inhibitors Zolinza (SAHA), Beleodaq (belinostat/PXD101), Farydak (panobinostat), and class I selective HDAC inhibitor Istodax (romidepsin) to treat peripheral or cutaneous T-cell lymphoma and multiple myeloma.[5] While HDAC inhibition is a promising therapeutic strategy, HDACs play essential roles in normal cellular function.[6] It has been hypothesized that HDAC isoform selective inhibitors would have improved efficacy and minimal adverse effects; thus, isoform selective compounds have been developed (for review see ref.[7]). In general, inhibition of class I HDAC isoforms and in some cases HDAC6, a class II isoform, is associated with anti-cancer activity.[8] For instance, it has been shown that overexpression of class I HDACs is correlated with a decrease in overall survival in prostate,[9] colon,[10] breast,[11] lung,[12] liver,[13] gastric,[14] and neuronal[15] cancers and that class I HDAC isoforms play predominant roles in epigenetic repression of key tumor suppressor genes and genes

involved in DNA damage repair in several tumor types.[8a, 16] Despite significant progress, many aspects of HDAC biology are not well characterized or understood. Among them are the role of individual HDAC isoforms in disease, the actual engagement of HDAC isoforms with inhibitors in vivo, or the compensatory action of one isoform for another when one isoform or a set of isoforms is inhibited. Likely for these reasons, the therapeutic application of HDAC inhibitors remains somewhat limited. Therefore, discovery of novel potent class I HDAC inhibitors, especially those with superior medicinal chemistry and anticancer properties, remains an important task for development of epigenetics-based therapeutics.

One of the key features of the binding site in the class I and II HDAC isoforms is an aspartic amino acid Asp104 (in HDAC2, different number in other HDACs) located at the gorge region of the binding site. The acidic side chain of this well conserved residue may be considered a “hot-spot” in the HDAC binding site. Being relatively solvent exposed, Asp104 is expected to be deprotonated, yet its protonation state and its precise role in binding inhibitors and histone substrates remains a matter of debate.[17] To probe the interaction between the Asp104 “hot spot” and ligands, we designed and synthesized a series of compounds with an aliphatic amino group as a part of their surface binding group (SBG, Figure 1). Although several HDAC inhibitor scaffolds containing a basic nitrogen have been explored,[18] there is no systematic investigation of the effect secondary and tertiary amines in the SBG may have on potency and HDAC isoform selectivity. To minimize the effect of the remaining portion of the ligands on the structure activity relationship (SAR), we focused our studies on compounds with the same linker and zinc binding group (ZBG, Figure 1). In our recent publication, we have already determined that the linker consisting of six methylene groups results in inhibitors more potent than those with a shorter linker.[19] The hydroxamic acid and ortho-aminoanilide moieties are the two ZBGs (Figure 1) most commonly used for HDAC inhibitor design. Hydroxamic acid is also present in the FDA approved HDAC inhibitors. The advantages and disadvantages of both ZBGs remain an area of active investigation.[20] Unlike the hydroxamic acid ZBG, however, the ortho-aminoanilide ZBG is known to skew inhibition toward HDAC1-3 isoforms.[21] To minimize potential bias of ortho-aminoanilide ZBG on SAR, we centered our efforts on hydroxamic acid-based compounds. In this paper, we report the design, synthesis, docking, inhibition of recombinant class I and cellular HDAC isoforms, biological evaluation in cellular models of cancer, and preliminary drug metabolism and pharmacokinetic studies of a novel series of HDAC inhibitors containing either secondary or tertiary aliphatic amino group as their SBG.

Results and Discussion

The synthesis of all the compounds is shown in Scheme 1 and the structures of the substituents R^1 and R^2 are shown in Table 1. The synthesis of the secondary and tertiary amine-based HDAC inhibitors is based on a reductive amination procedure, which has been described by us and others.[22] A small library of commercially available aromatic aldehydes **1a–m** were reacted with methyl 7-aminoheptanoate. The resulting secondary and tertiary amines **6a–m** and **7a–m**, respectively, were isolated and purified. The subsequent treatment of **6a–m** and **7a–m** with NH_2OH in MeOH gave the target hydroxamic acids **2a–m** and **3a–m** (Scheme 1).

Considering the importance of inhibition of class I isoforms in cancer, we mainly focused on testing the inhibitory activity against HDAC isoforms 1, 2, 3, and 8. A representative set of amine-based inhibitors was also tested in cells for inhibition of acetylation of α-tubulin, a well validated cellular target of HDAC6. The IC_{50} values of amines **2a–m** and **3a–m** for deacetylase activity of class I HDACs are shown in Table 1. They were determined using a competitive fluorescence-based assay similar to that previously reported by us.[23] Briefly, the inhibition of HDAC1, 2, and 3 was measured using the fluorescent HDAC substrate Boc-L-Lys(Ac)-AMC and commercially available recombinant human HDAC1, 2, and 3 expressed in baculovirus expression system, whereas the inhibition of HDAC8 was measured using the commercially available HDAC substrate and purified recombinant human HDAC8 from *Escherichia coli*.[24]

We found that replacement of the amide moiety in SAHA (**1**) to an amino group in amine **2a** led to a 8- to 40-fold decrease in potency against all class 1 HDACs to 340, 3100, 430, and 1800 nM, respectively (Table 1). To investigate how substitution of the aromatic ring in **2a** with electron withdrawing groups (EWGs) and/or electron donating groups (EDGs) would affect potency, we synthesized and screened secondary amines **2b–e**.

Overall, the potency and the pattern of HDAC isoform inhibition were only moderately affected by addition of EWGs and/or EDGs compared to those of **2a**. For amines **2b–e**, the potency for HDAC1 ranged from 140–220 nM, HDAC2 – 790–2900 nM, HDAC3 – 180–1000 nM, and HDAC8 – 1700–2800 nM. No particular EWG- or EDG-dependent trend was observed. Introduction of these substituents in amines **2b–e** generally resulted in a moderate improvement in potency against HDAC1, 2, and 3 and less than 30% change in potency against HDAC8. Specifically, introduction of *p*-NO_2 in **2b**, *p*-fluoro in **2c**, *p*-fluoro and *m*-CH_3 in **2d**, and *m*,*p*-OCH_3 in **2e** improved HDAC1 potency of these compounds from 340 nM for amine **2a** to 220, 220, 140, and 210 nM, respectively. HDAC2 potency also showed only a moderate improvement from 3100 nM for **2a** to 2900, 1500, 790, and 1800 nM for **2b–e**, respectively. For compound **2b**, potency against HDAC3 showed a 2.3-fold decrease, whereas for compounds **2c–e** potency improved to 240, 190, and 180 nM, respectively. Potency against HDAC8 remained in the single digit micromolar range – 2100, 1700, 2800, and 1800 nM for **2b–e**, respectively.

The introduction of EWG and EDG substituents in amines **2b–e** had either slightly improved class I HDAC isoform selectivity or had no effect. The presence of the *p*-nitro group, a strong EWG, moderately improved the selectivity of **2b** towards HDAC1, whereas a combination of *p*-fluoro and *m*-methyl substituents, a weak EDG and an EWG, respectively, made compound **2d** more selective for HDAC1, 2, and 3 over HDAC8. The selectivity of **2c** and **2e** remained relatively comparable with **2a**; that is, selective for HDAC1 and 3 over HDAC2 and 8.

Next, we explored how changes in the size, lipophilicity, and polarity of the SBG substituents would affect activity of the ligands (Table 1). The pyridine ring in amine **2f** had little effect on HDAC inhibition compared to that of amine **2a**, 430, 3200, 310, and 1600 nM for HDAC1, 2, 3, and 8, respectively. Replacement of the phenyl ring in **2a** with fused bicyclic moieties naphthyl, methylenedioxophenyl, *N*-substituted indole, and indole in **2g–j**,

respectively, had by far the most robust effect on improvement of the potency for all class I HDAC isoforms. Potency of compounds **2g–j** for HDAC1 was 39, 130, 250, and 61 nM, HDAC2 – 320, 840, 1800, and 260 nM, HDAC3 – 68, 170, 120, and 25 nM, and HDAC8 – 320, 270, 720, and 620 nM, respectively. The selectivity profile for **2g–j** was similar to amine **2a** (Table 2). Replacement of the phenyl ring in **2a** with bi-aryl substituents in amines **2k** and **2l** had an effect similar to that found in the amines with bicyclic substituents. These compounds were superior to amine **2a** and maintained the overall HDAC isoform selectivity profile. Specifically, placement of a pyridine ring in the para position of the phenyl group in amine **2k** resulted in an improvement in IC_{50} for all class I HDACs in comparison to compound **2a** (Tables 1 and 2), 130, 620, 160, and 800 nM for HDAC1, 2, 3, and 8, respectively. Introduction of a bicyclic ring system of thiophene had resulted in potent and selective HDAC1 and 3 inhibitor **2l** (Table 1 and 2). The values of IC_{50} against HDAC1 and 3 for **2l** were 48 and 38 nM, respectively. The selectivity profile of **2l** had shown 11 to 14-fold difference in inhibition between HDAC1 and 3 versus HDAC2 and 8 (Table 2). Introduction of a longer SBG in amine **2m** resulted in a substantial loss of activity - 1500, 3000, 1500, and 2500 nM, for HDAC1, 2, 3, and 8, respectively.

We also synthesized the corresponding tertiary amines and found that, with few exceptions, their potency varied from single to double digit micromolar. An introduction of an additional tertiary substituent in amines **3a–d** and **3h–l** had resulted in less potent inhibitors than the corresponding secondary amines (Table 1). The effect of the size, lipophilicity, and polarity was rather unpronounced compared to that of the secondary amines. In the case of 3,4-dimethoxy and 3-pyridine substituents, however, additional SBGs in amines **3e** and **3f** did not cause any significant changes in their potency and resulted in an inhibitory profile similar to that of the corresponding secondary amines **2e** and **2f** (Table 1). In **3i** and **3j**, the additional methylenedioxophenyl, *N*-substituted indole and indole moieties have resulted in compounds more potent against HDAC1 in comparison with the corresponding secondary amines (Table 1 and Table 2). Potency of compounds **3i** and **3j** for HDAC1 was 680 and 340 nM, HDAC2 – 3700 nM, HDAC3 – 2900 and 1300 nM, and HDAC8 – 2100 and 4600 nM, respectively. In **3m**, the additional long linear substituent resulted in almost no changes in potency against HDAC1 and 3 and a 2.2- and 10-fold decrease in potency against HDAC2 and 8, respectively, compared to corresponding secondary amine **2m**. Among the tertiary amines, **3e** was the most potent inhibitor with IC_{50} of 270, 1100, 290, and 2100 nM against HDAC1, 2, 3, and 8, respectively. In contrast to secondary amine **2l** that was more selective for HDAC1 and 3, tertiary amines **3i** and **3j** were more selective toward HDAC1 and tertiary amine **3k** was more selective toward HDAC3 (Table 2).

We have previously demonstrated that tertiary amine-based HDAC inhibitors can be converted to photoreactive probes **P1** and **P2** (Figure 2A) by introducing a photoreactive 3-azido-5-azidomethylene benzyl moiety as one of the substituents at the basic nitrogen atom and the other substituents are either an indole group (**P1**) or a 5-(4-tert-butoxycarbonylaminophenyl) isoxazole group (**P2**).[25] We used these probes as nanorulers to determine the distance between the catalytic site of HDAC3 and its co-activator silencing mediator of retinoid and thyroid hormone receptors (SMRT-DAD). Given the observed difference in potency of the SBGs in pairs **2j**/**3j** and **2m**/**3m** (Table 1), we sought to

determine the effect of placing two different groups on the inhibitory profile and if this modification affects their binding and/or suitability for photolabeling experiments against other class I HDACs. Probes **P1** and **P2** displayed moderate potency (Figure 2A) against class I HDAC isoform, which is in agreement with the potency for the other tertiary amines reported here. Potency of **P1** and **P2** for HDAC1 was 2300 and 1200 nM, HDAC2 – 4700 and 5600 nM, HDAC3 – 890 and 590 nM, and HDAC8 – 6000 and 14000 nM, respectively (Figure 2A). The introduction of 3-azido-5-azidomethylene benzyl moiety in **P1** and **P2** has resulted in a better inhibitory profile toward HDAC3 with at least 2-fold increase in potency between HDAC1 and 3 and 5–23 fold increase between HDAC3 and HDAC2 and 8. These results suggest that introduction of any bulky tertiary substituent leads to an overall lower activity. The improved potency of **P1** and **P2** suggests that further improvement of potency and selectivity of tertiary amines **3** can be achieved upon additional SAR studies but is unlikely to be substantial. Next, we performed the photolabeling experiments with probes **P1** and **P2**. In this type of photoreactive probes, the aromatic azide is used to generate a reactive nitrene upon UV irradiation thereby forming covalent adducts with HDACs, whereas the aliphatic azide reacts with a reporter tag, e.g. the biotin-containing tag shown in Figure 2A, via a “click-chemistry” reaction.[23, 25–26] At a fixed concentration of 8.5 μM, both **P1** and **P2** can label recombinant HDAC1 and 8 (Figure 2B, 2C), whereas the labeling of HDAC3 was demonstrated previously.[25] Only a marginal and likely non-specific biotinylation of HDAC1 and 8 is observed in the experiments where the proteins were preincubated with 42.5 μM of trichostatin A (TSA), a non-selective HDAC inhibitor. Overall, these experiments demonstrate that **P1** and **P2** can be used as photolabeling probes against all class I HDACs and, hence, represent additional tools for future target engagement and target identification experiments in live cells for class I HDACs.[27]

To gain additional structural insights into the SAR, amines **2** and **3** were docked to HDAC2 (PDB: 4LXZ[28]) using Molecular Operating Environment (MOE) software.[29] The top docking poses of two representative amines **2j** and **3e** are shown in Figure 3A and 3B, respectively. A 2D map of the interactions of these ligands with HDAC2 is shown in Figure 4. An analysis of the docking poses shows that the SBG of the secondary amines occupies one of the hydrophobic grooves and forms a salt bridge between the charged secondary amino group of the ligands and Asp104 of HDAC2. Amines with basic nitrogen atoms in the SBG may form an additional polar interaction with Glu103 similar to that shown for **2j** in Figure 3A and 4A. The exact placement of the aryl substituents in the binding site depends on their size, shape, and electronic properties. It tends to gravitate to the poses with the largest area of contact with the hydrophobic portions of the binding site and, whenever possible, a salt bridge between the charged amino group and the ionized side chain of Asp104. Considering our previous studies and availability of multiple conformations with similar scores for the docked amine-based inhibitors,[30] binding of these compounds as an ensemble of poses rather than a single pose cannot be excluded. The former would also result in a smaller loss in entropy and, hence, better binding. For systems similar to amines **2** and **3** bound to HDACs, salt bridges were shown to contribute on average 12–21 kJ/mol to the protein stabilization energy,[31] which is notably more than the typical 5.0 ± 2.5 kJ/mol contribution of a hydrogen bond to the binding.[32] Despite the possible advantage of having a salt bridge between the protonated amino group of the ligands and deprotonated side chain

of Asp104 compared to a hydrogen bond between these groups in a neutral form, it is unclear if this is the case. The fact that all the secondary amines **2**, even a nearly identical to **1** amine **2a**, are less potent than **1** suggests that the charged amino group does not gain free energy of binding comparable to that of **1** likely due to a higher overall solvation-desolvation penalty. The docking of tertiary amines **3** shows that in all the poses both the substituents share a rather narrow gorge of the binding site, which likely results in a large entropic loss. Only one methylene spacer between the amino group and the aryl group offers a very limited set of conformations, if any, in which both the substituents can form enthalpically favorable interactions with the binding site. Moreover, tertiary amines **3** are limited in their choice between a binding pose where there is a salt-bridge with Asp104 and marginal interaction between the aromatic substituents and the lipophilic portion of the binding site as shown for **3e** (Figures 3B and 4B) and a conformation where the aromatic substituents (or at least one of them) form pronounced interaction with the hydrophobic area of the binding site whereas the distance between the negative side chains of Asp104 and Glu103 and positively charged tertiary amine is extended to at least 5–6 Å. Lacking additional bulky tertiary substituent, secondary amines **2** are much less restricted in their poses and maintain both these interactions with the binding site simultaneously. These observations suggest that both the higher entropic loss and the smaller enthalpic gain upon binding of tertiary amines **3** are likely the reasons they are less potent than corresponding secondary amines **2**.

In silico druglike properties of amine-based HDAC inhibitors were calculated in MOE and included water/octanol partition coefficient Slog*P* and water/octanol distribution coefficient at pH 7 log*D* as descriptors of lipophilicity, solubility log*S*, and topological surface area TPSA. The lipophilic ligand efficiency LLE was calculated as reported by Ryckmans et al[34] in QikProp/Schrödinger software.[35] An analysis of the calculated log*P*, log*S*, TPSA, MW, log*D*, and LLE given in Table 3 indicates that the secondary and tertiary amines are generally leadlike/druglike and are excellent starting point for further drug discovery efforts.[36] Low molecular weight, TPSA below 90 Å, presence of a basic aliphatic nitrogen atom, log*D* in the range of 0–3, and a number of nitrogen and oxygen atoms below 5 suggest that these compounds have high probability to be brain-blood barrier (BBB) permeable.[37] The majority of potent secondary amines **2** are characterized by LLE above 4 and calculated log*P* between 2 and 3, indicating that these compounds are likely to have acceptable ADME properties.[38] Additionally, *in silico* evaluation of secondary and tertiary amines activity against hERG potassium channel, a predictor of QT prolongation and cardiac toxicity,[39] were performed using QikProp/Schrödinger software (Table 3).[35] In all the cases, secondary amines **2** were found to be less potent against hERG than the corresponding amines **3**. With few exceptions, the secondary and tertiary amine-based inhibitors displayed acceptable (greater than −5) predicted logIC_{50} for hERG activity.

Next, a representative set of seven amine-based inhibitors **2g**, **2h**, **2j–l**, **3e**, and **3f** and the parent compound **1** were tested for antiproliferative activities against three cancer cell lines of human origin: colorectal adenocarcinoma HT-29, neuroblastoma SH-SY5Y, and breast adenocarcinoma MFC-7, using an alamarBlue assay.[40] The EC_{50} against HT-29 and SH-SY5Y cells and percent growth inhibition at 10 μM against MCF-7 cells are shown in Table 4. The EC_{50} were measured at 24 and 48 hours. In case of HT-29 cells, the EC_{50} at 24 hours

for **1** and all the amines tested were above 50 μM, except for compounds **2k** and **2l** exhibiting EC_{50} of 35 μM and 24 μM, respectively. At 48 h, EC_{50} against HT-29 cells for **1** and amines **3e**, **2g**, **2h**, and **2j–l** were in the range between 1.1 μM and 4.2 μM with compound **2g** being the most potent with an EC_{50} of 1.1 μM. Amine **3f** was ineffective against HT-29 cells even at 48 h time point. In case of SH-SY5Y cells, the EC_{50} at 24 h for **1** and amines **2g**, **2h**, **2j**, **3e**, and **3f** were above 50 μM. Amines **2k** and **2l** displayed EC_{50} of 13 and 15 μM, respectively. At 48 h, EC_{50} for **1** and all the amines tested ranged between 1.2 to 23 μM. Potency of amines **2g** and **2j** was superior to that of **1**, 1.2 and 1.3 μM, respectively. Except for amine **3f** that exhibited EC_{50} of only 23 μM, potency of other amines was either comparable or somewhat lower than that of **1**. In case of MCF-7, the calculated percentage of inhibition at 24 h for 10 μM of **1** and amines **2j–l** and **3e** was 48%, 61%, 66%, 63%, and 55%, respectively, whereas amines **2g**, **2h**, and **3f** displayed less than 25% of inhibition. At 48 h, the percent of inhibition by amines **2g**, **2h**, **2j–l**, and **3e** was above 46%. Amines **2j** and **2l**, both with 71% of inhibition, were found to be slightly more potent than **1**, which exhibited 69% of inhibition. Amine **3f**, on the other hand, was almost inactive and displayed only an 8.7% inhibition of MCF-7 cells growth. These results show that secondary amine-based HDAC inhibitors have comparable or in some cases better cytotoxicity profile than that of **1**.

To enable analysis of the correlation between the activity of these compounds against recombinant enzymes and the cytotoxicity data, we calculated the correlation coefficients (R) between all the IC_{50} and EC_{50} at 48 h for the compounds in Table 4. The complete data are given in Supplementary Figure 1. The IC_{50} values for HDAC1, 2, and 3 are highly correlative, with correlation coefficient R ranging between 0.91 and 0.99. Considering very high homology between the sequences of HDAC1, 2, and 3, such high correlation observed between the potencies against these enzymes appears to be reasonable. Correlation of IC_{50} for HDAC1, 2, and 3 with those of HDAC8, a less homologous isoform, is lower, with R of 0.75, 0.53, and 0.73, respectively. A similar correlation analysis of IC_{50} values for each individual isoform and EC_{50} against HT-29 and SH-SY5Y cells shows a strong correlation between inhibition of HDAC1, 2, and 3 isoforms and cytotoxicity, with R ranging between 0.81 and 0.98. The R for the correlation between EC_{50} against HT-29 and SH-SY5Y cells and IC_{50} for HDAC8 is 0.43 for both cell lines. These data suggest that the cytotoxicity stems largely from inhibition of either individual HDAC isoform 1, 2, and 3 or their combinations. The correlation coefficient between cytotoxicity for both cell lines and activity against HDAC2 was found to be somewhat higher, 0.98, compared to that for the other combinations of the isoforms and the cell lines. Strong intercorrelation between IC_{50} values for HDAC1, 2, and 3 does not allow to identify a particular isoform(s) primarily responsible for cytotoxicity. Removal of amines **2l** and **3f**, two compounds with very poor EC_{50} values that can artificially improve correlation, has resulted in generally similar correlation. Interestingly, it also resulted in substantial improvement in correlation with IC_{50} for HDAC8, 0.93 and 0.78 for HT-29 and SH-SY5Y, respectively. The presence of thiophene ring, which is a known metabolic liability, in amine **2l** and differences in bioenergetics between SH-SY5Y and HT-29 cells may account for lower than expected (based on its HDAC inhibitory profile) cytotoxicity of amine **2l** in SH-SY5Y cells. Alternatively, poor cell permeability or precipitation of **2l** and **3f**, although the latter was not observed upon visual

inspection, may also affect their potency in cell-based assays. To determine whether this may be the case, we compared log*P*, log*S*, and TPSA parameters for all compounds in this series (Table 3). We found that for both **2l** and **3f** these parameters were similar to those of the other compounds tested for cell-based cytotoxicity, with compound **2l** having the lowest calculated solubility logS of −4.41. It suggests that at least in case of **2l** solubility may potentially affect its activity in cell-based assays.

Next, we sought to validate acetylation of histones 3 (H3) and 4 (H4) as the target for amines **2e**, **2g**, **2h**, **2j**, **2k**, **3f**, and **3k** in HT-29 and SH-SY5Y cells by Western blot (Figure 5 and 6). Compound **1** was used as a positive control. In HT-29 cells, the acetylation was measured at preincubation times of 6 and 24 hours and at a concentration of 5 μM for all the compounds. These preincubation times and the subtoxic dose for the inhibitors were selected to ensure that the effect of inhibition is mediated by engaging the target while most cells are still alive. At 6 h, compound **1** and amines **2e**, **2g**, **2h**, **2j**, **2k**, **3f**, and **3k** increased the acetylation level of H3 and only compound **2g** was able to significantly increase acetylation of H4 (Figure 5A). At 24 h, a time-dependent increase in acetylation of H3 and H4 was observed for amines **2e**, **2g**, **2h**, and **2j**, and in H4 only for **2k** (Figure 5B). Compounds **1**, **3f**, and **3k** were unable to cause any significant time-dependent increase in acetyl H3 and acetyl H4. The inability of **1** to further increase acetylation of H3 and H4 at 24 h in HT-29 cells prompted us to investigate the acetylation patterns in SH-SY5Y cells under same conditions (Figure 6). At 6 h, the acetylation of both H3 and H4 was increased by compound **1** and amines **2e**, **2g**, **2h**, **2j**, **2k**, **3f**, and **3k** (Figure 6A). At 24 h, a time-dependent increase in acetylation of H3 and H4 was observed for **2e**, **2g**, **2h**, **2j**, **2k**, **3k**, and **1**, except for **3f** (Figure 6B). Overall, the ability of compounds to increase acetylation of H3 and H4 supports the correlation between the IC_{50} values against HDAC1, 2, and 3 and the cytotoxic effects in HT-29 and SH-SY5Y cells (Supplementary Figure 1B), which is consistent with our previous observations and those from other laboratories.[4d, 19, 41] The differences in the global hyperacetylation state in H3 and H4 at 24 h time point in HT-29 and SH-SY5Y cells in response to the treatment with **1** indicate that its cytotoxic effect may be mediated via cell type-dependent mechanisms that may involve non-histone targets as well. In fact, multiple modes of action of **1** in HT-29 and other colorectal cancer cell lines were observed by other groups.[42] This finding warrants further investigation into the mode of action of **1** and other HDAC inhibitors in different cell lines for additional target identification.

To determine if inhibition of class II HDACs, specifically HDAC6, by amines **2** and **3** can also contribute to cytotoxicity, we determined their effect on acetylation of α-tubulin, a known cytosolic substrate of HDAC6. At 6 h, compound **1** and amines **2e**, **2g**, **2h**, **2j**, **2k**, and **3f** increased the acetylation level of α-tubulin in HT-29 cell lines, whereas amine **3k** showed only a small and not statistically significant increase (Figure 7A). At the same time point, amines **2g**, **2h**, **2j**, **2k**, **3f**, and **3k** and compound **1** increased the acetylation of α-tubulin in SH-SY5Y cells. Amine **2e** showed moderate but not a statistically significant increase. At 24 h, a time-dependent increase in acetylation of α-tubulin in HT-29 cells was observed only for amine **2j** and **1** (Figure 7B). Unlike **1**, none of the amines tested induced statistically significant acetylation of α-tubulin in SH-SY5Y cells at 24 h. To investigate this further, we determined the HDAC6 inhibitory activity of a representative secondary amine **2j**

and found it to be a potent inhibitor of HDAC6 with an IC_{50} of 67 nM (Table 1, Supplementary Figure 2). Similar tertiary amine-based HDAC inhibitors have been reported to be potent HDAC6 inhibitors as well.[19] These data suggest that the amine-based HDAC inhibitors may inhibit HDAC6 transiently in cells, displaying a different time-dependent inhibitory profile compared to **1**. Considering similar structure and HDAC inhibitory profiles of compound **1** and amines **2** and **3**, the apparent time-dependent effect is likely due to the presence of a basic aliphatic amino group in amines **2** and **3**. The continuous acetylation of H3 and H4, nuclear targets for class I HDACs, and the temporary hyperacetylation of α-tubulin, a cytosolic target for HDAC6, suggest that the amine-based inhibitors **2** and **3** accumulate in a time-dependent manner in the nucleus and possibly other organelles leading to a decrease in concentration in the cytosol. Although further studies are needed to determine the origin of these observations, one of the plausible explanations is a pK_a/pH-dependent sequestration of amines into cellular compartments/organelles that was previously reported for unrelated small molecules.[43]

Next, we conducted a preliminary study where we measured rat liver (RLM) and human liver (HLM) microsomal stability and rat blood brain barrier (BBB) permeability of amine **2j**. This compound was selected based on its superior potency against class I HDACs, cytotoxicity against HT-29, SH-SY5Y, and MCF7 cells, and robust effect on acetylation of H3, H4, and α-tubulin. Two potential alternative candidates, amines **2g** and **2l**, were deprioritized based on their lower average IC_{50} values for HDAC1, 2, and 3 and lower predicted solubility logS (Table 3). The plasma concentration and BBB permeability were assessed at 20 and 40 min after i.p. administration of 25 mg/kg of **2j**. Plasma levels of **2j** were 3820 ± 2050 ng/mL and 2100 ± 720 ng/mL and rat brain levels of **2j** were 122 ± 21 ng/mL and 107 ± 15 ng/mL at 20 and 40 min, respectively (Figure 8). At 20 min, the corresponding molar concentrations were 14 μM and 0.41 μM in plasma and brain, respectively. This plasma concentration is 230-, 54-, 560-, and 23-fold higher than the IC_{50} values for HDAC1, 2, 3, and 8, respectively (Table 1). The concentration in the brain is lower than that in plasma but still 6.7-, 1.6-, and 16-fold above the IC_{50} values for HDAC1, 2, and 3, respectively (Table 1). The results of the microsomal stabilities of amine **2j** in RLM and HLM are summarized in Figure 9. Pronounced differences were found in stability of amine **2j** between species. We found that **2j** is more stable in RLM, with 85% left after 30 min, than in HLM, with only 12% left after 30 min incubation (Figure 9), suggesting that stability of amine **2j** may be affected by first-pass metabolism in humans. Despite the somewhat moderate stability of compound **2j**, the plasma and brain availability data in rats indicate that amines are highly bioavailable and are promising candidates for further development for a variety of therapeutic applications.

Conclusions

In summary, a novel series of secondary and tertiary amine-based HDAC inhibitors **2a–m** and **3a–m** was designed, synthesized, and characterized in a variety of biochemical and cellular assays. Secondary amines **2** were found to be generally more potent than the corresponding tertiary amines **3**. Addition of fused or bicyclic substituents was found to result in more potent inhibitors, whereas small electron withdrawing and donating

substituents had little effect on potency. Compounds **2g**, **2j**, and **2l** were particularly potent and superior to almost all other compounds in this series. Inhibitors **2j/3j** and **2m/3m** were converted to corresponding photoreactive probes **P1** and **P2** and their inhibitory profile and suitability for photolabeling experiments were investigated. Both probes showed improved potency against HDAC3 in comparison to HDAC1, 2, and 8 and successfully labeled recombinant HDAC1, 3, and 8, warranting their application for target engagement studies in live cells. Docking of the amine-based inhibitors to HDAC2 showed that the SBG in amines **2** occupies one of the hydrophobic grooves and forms a salt bridge with Asp104 while maximizing the area of contact with the hydrophobic portions of the binding site. Generally lower activity of tertiary amines **3** is likely associated with the higher entropic loss and smaller enthalpic gain due to unfavorable accommodation of the larger SBG at the gorge region of the binding site. Compounds **2g**, **2h**, **2j–l**, **3e**, and **3f** were tested for cytotoxicity against HT-29, SH-SY5Y, and MCF-7 cells, and displayed single digit micromolar EC_{50} values that correlated with inhibition of class I HDACs. Further assessment of the acetylation pattern in HT-29 and SH-SY5Y cells confirmed that cytotoxicity was likely due to the global hyperacetylation of H3, H4, and α-tubulin. The time-dependent increase in acetylation of H3 and H4, but not α-tubulin, suggests that the amine-based inhibitors **2** and **3** may accumulate in the nuclei of cells, leading to a continuous inhibition of HDAC1, 2, and 3 and an effective decrease in inhibition of HDAC6. Amine **2j** was found to be metabolically stable in rats and achieved concentrations in plasma and brain well above its IC_{50} for class I HDACs. Overall, compounds in this series display excellent therapeutic capacity for a variety of anti-cancer applications.

Supplementary Material

Refer to Web version on PubMed Central for supplementary material.

Acknowledgments

This study was funded by the National Cancer Institute/NIH grants R21 CA183627, R01 CA131970, R01 HL130760, and the Alzheimer's Drug Discovery Foundation grant ADDF #20101103.

References

1. Haberland M, Montgomery RL, Olson EN. Nat. Rev. Genet. 2009; 10:32–42. [PubMed: 19065135]
2. a) Jenuwein T, Allis CD. Science. 2001; 293:1074–1080. [PubMed: 11498575] b) Gardner KE, Allis CD, Strahl BD. J. Mol. Biol. 2011; 409:36–46. [PubMed: 21272588]
3. a) Delcuve GP, Khan DH, Davie JR. Clin. Epigenet. 2012; 4:5.b) Xu WS, Parmigiani RB, Marks PA. Oncogene. 2007; 26:5541–5552. [PubMed: 17694093]
4. a) Falkenberg KJ, Johnstone RW. Nat. Rev. Drug Discovery. 2014; 13:673–691. [PubMed: 25131830] b) Glaser KB, Staver MJ, Waring JF, Stender J, Ulrich RG, Davidsen SK. Mol. Cancer Ther. 2003; 2:151–163. [PubMed: 12589032] c) Johnstone RW. Nat. Rev. Drug Discovery. 2002; 1:287–299. [PubMed: 12120280] d) Marks P, Rifkind RA, Richon VM, Breslow R, Miller T, Kelly WK. Nat. Rev. Cancer. 2001; 1:194–202. [PubMed: 11902574] e) Minucci S, Pelicci PG. Nat. Rev. Cancer. 2006; 6:38–51. [PubMed: 16397526] f) Robert T, Vanoli F, Chiolo I, Shubassi G, Bernstein KA, Rothstein R, Botrugno OA, Parazzoli D, Oldani A, Minucci S, Foiani M. Nature. 2011; 471:74–79. [PubMed: 21368826] g) Li Z, Zhu WG. Int. J. Biol. Sci. 2014; 10:757–770. [PubMed: 25013383]

5. a) Kim HJ, Bae SC. Am. J. Transl. Res. 2011; 3:166–179. [PubMed: 21416059] b) Giannini G, Cabri W, Fattorusso C, Rodriquez M. Future Med. Chem. 2012; 4:1439–1460. [PubMed: 22857533] c) Grasso CS, Tang Y, Truffaux N, Berlow NE, Liu L, Debily MA, Quist MJ, Davis LE, Huang EC, Woo PJ, Ponnuswami A, Chen S, Johung TB, Sun W, Kogiso M, Du Y, Qi L, Huang Y, Hutt-Cabezas M, Warren KE, Le Dret L, Meltzer PS, Mao H, Quezado M, van Vuurden DG, Abraham J, Fouladi M, Svalina MN, Wang N, Hawkins C, Nazarian J, Alonso MM, Raabe EH, Hulleman E, Spellman PT, Li XN, Keller C, Pal R, Grill J, Monje M. Nat. Med. 2015; 21:827.
6. Reichert N, Choukrallah MA, Matthias P. Cell. Mol. Life Sci. 2012; 69:2173–2187. [PubMed: 22286122]
7. a) Falkenberg KJ, Johnstone RW. Nat. Rev. Drug Discovery. 2015; 14:219–219. [PubMed: 25656595] b) Thaler F, Mercurio C. Chem Med Chem. 2014; 9:523–526. [PubMed: 24730063]
8. a) West AC, Johnstone RW. J. Clin. Invest. 2014; 124:30–39. [PubMed: 24382387] b) Witt O, Deubzer HE, Milde T, Oehme I. Cancer Lett. 2009; 277:8–21. [PubMed: 18824292]
9. Weichert W, Roske A, Gekeler V, Beckers T, Stephan C, Jung K, Fritzsche FR, Niesporek S, Denkert C, Dietel M, Kristiansen G. Br. J. Cancer. 2008; 98:604–610. [PubMed: 18212746]
10. Weichert W, Roske A, Niesporek S, Noske A, Buckendahl AC, Dietel M, Gekeler V, Boehm M, Beckers T, Denkert C. Clin. Cancer Res. 2008; 14:1669–1677. [PubMed: 18347167]
11. a) Muller BM, Jana L, Kasajima A, Lehmann A, Prinzler J, Budczies J, Winzer KJ, Dietel M, Weichert W, Denkert C. BMC Cancer. 2013; 13:215. [PubMed: 23627572] b) Krusche CA, Wulfing P, Kersting C, Vloet A, Bocker W, Kiesel L, Beier HM, Alfer J. Breast Cancer Res. Treat. 2005; 90:15–23. [PubMed: 15770522]
12. Minamiya Y, Ono T, Saito H, Takahashi N, Ito M, Mitsui M, Motoyama S, Ogawa J. Lung Cancer. 2011; 74:300–304. [PubMed: 21466904]
13. Rikimaru T, Taketomi A, Yamashita Y, Shirabe K, Hamatsu T, Shimada M, Maehara Y. Oncology. 2007; 72:69–74. [PubMed: 18004079]
14. Weichert W, Roske A, Gekeler V, Beckers T, Ebert MP, Pross M, Dietel M, Denkert C, Rocken C. Lancet Oncol. 2008; 9:139–148. [PubMed: 18207460]
15. Oehme I, Deubzer HE, Lodrini M, Milde T, Witt O. Expert Opin. Investig. Drugs. 2009; 18:1605–1617.
16. a) Glozak MA, Seto E. Oncogene. 2007; 26:5420–5432. [PubMed: 17694083] b) Eot-Houllier G, Fulcrand G, Magnaghi-Jaulin L, Jaulin C. Cancer Lett. 2009; 274:169–176. [PubMed: 18635312]
17. a) Vannini A, Volpari C, Gallinari P, Jones P, Mattu M, Carfi A, De Francesco R, Steinkuhler C, Di Marco S. EMBO Rep. 2007; 8:879–884. [PubMed: 17721440] b) Dowling DP, Gantt SL, Gattis SG, Fierke CA, Christianson DW. Biochemistry. 2008; 47:13554–13563. [PubMed: 19053282]
18. a) Zhou M, Ning C, Liu R, He Y, Yu N. Bioorg. Med. Chem. Lett. 2013; 23:3200–3203. [PubMed: 23639537] b) Terracciano S, Chini MG, Riccio R, Bruno I, Bifulco G. Chem Med Chem. 2012; 7:694–702. [PubMed: 22278987] c) Remiszewski SW, Sambucetti LC, Bair KW, Bontempo J, Cesarz D, Chandramouli N, Chen R, Cheung M, Cornell-Kennon S, Dean K, Diamantidis G, France D, Green MA, Howell KL, Kashi R, Kwon P, Lassota P, Martin MS, Mou Y, Perez LB, Sharma S, Smith T, Sorensen E, Taplin F, Trogani N, Versace R, Walker H, Weltchek-Engler S, Wood A, Wu A, Atadja P. J. Med. Chem. 2003; 46:4609–4624. [PubMed: 14521422] d) Attenni B, Ontoria JM, Cruz JC, Rowley M, Schultz-Fademrecht C, Steinkuhler C, Jones P. Bioorg. Med. Chem. Lett. 2009; 19:3081–3084. [PubMed: 19410459] e) Zhang L, Zhang Y, Chou CJ, Inks ES, Wang X, Li X, Hou J, Xu W. Chem Med Chem. 2014; 9:638–648. [PubMed: 24227760] f) Su H, Yu L, Nebbioso A, Carafa V, Chen Y, Altucci L, You Q. Bioorg Med. Chem. Lett. 2009; 19:6284–6288. [PubMed: 19822426] g) Marson CM, Mahadevan T, Dines J, Sengmany S, Morrell JM, Alao JP, Joel SP, Vigushin DM, Charles Coombes R. Bioorg. Med. Chem. Lett. 2007; 17:136–141. [PubMed: 17046252]
19. Taha TY, Aboukhatwa SM, Knopp RC, Ikegaki N, Abdelkarim H, Neerasa J, Lu Y, Neelarapu R, Hanigan TW, Thatcher GRJ, Petukhov PA. ACS Med. Chem. Lett. 2017; 8:824–829. [PubMed: 28835796]
20. a) Shen S, Kozikowski AP. Chem Med Chem. 2016; 11:15–21. [PubMed: 26603496] b) Weiwer M, Lewis MC, Wagner FF, Holson EB. Future Med. Chem. 2013; 5:1491–1508. [PubMed: 24024943]

21. Vaidya AS, Karumudi B, Mendonca E, Madriaga A, Abdelkarim H, van Breemen RB, Petukhov PA. Bioorg. Med. Chem. Lett. 2012; 22:5025–5030. [PubMed: 22771007]
22. a) Abdel-Magid AF, Carson KG, Harris BD, Maryanoff CA, Shah RD. J. Org. Chem. 1996; 61:3849–3862. [PubMed: 11667239] b) Abdelmagid AF, Harris BD, Maryanoff CA. Synlett. 1994:81–83.c) Neelarapu R, Petukhov PA. Tetrahedron. 2012; 68:7056–7062. [PubMed: 22844160]
23. Neelarapu R, Holzle DL, Velaparthi S, Bai H, Brunsteiner M, Blond SY, Petukhov PA. J. Med. Chem. 2011; 54:4350–4364. [PubMed: 21548582]
24. Dowling DP, Gattis SG, Fierke CA, Christianson DW. Biochemistry. 2010; 49:5048–5056. [PubMed: 20545365]
25. Abdelkarim H, Brunsteiner M, Neelarapu R, Bai H, Madriaga A, van Breemen RB, Blond SY, Gaponenko V, Petukhov PA. ACS Chem. Biol. 2013; 8:2538–2549. [PubMed: 24010878]
26. a) He B, Velaparthi S, Pieffet G, Pennington C, Mahesh A, Holzle DL, Brunsteiner M, van Breemen R, Blond SY, Petukhov PA. J. Med. Chem. 2009; 52:7003–7013. [PubMed: 19886628] b) Vaidya AS, Karumudi B, Mendonca E, Madriaga A, Abdelkarim H, van Breemen RB, Petukhov PA. Bioorg. Med. Chem. Lett. 2012; 22:5025–5030. [PubMed: 22771007]
27. Hanigan TW, Aboukhatwa SM, Taha TY, Frasor J, Petukhov PA. Cell Chem. Biol. 2017
28. Lauffer BEL, Mintzer R, Fong R, Mukund S, Tam C, Zilberleyb I, Flicke B, Ritscher A, Fedorowicz G, Vallero R, Ortwine DF, Gunzner J, Modrusan Z, Neumann L, Koth CM, Lupardus PJ, Kaminker JS, Heise CE, Steiner P. J. Biol. Chem. 2013; 288:26926–26943. [PubMed: 23897821]
29. Molecular Operating Environment (MOE), 2016.0802. Chemical Computing Group Inc.; 1010 Sherbooke St. West, Suite #910, Montreal, QC, Canada: 2017. p. H3A 2R7
30. He B, Velaparthi S, Pieffet G, Pennington C, Mahesh A, Holzle DL, Brunsteiner M, van Breemen R, Blond SY, Petukhov PA. J. Med. Chem. 2009; 52:7003–7013. [PubMed: 19886628]
31. a) Anderson DE, Becktel WJ, Dahlquist FW. Biochemistry. 1990; 29:2403–2408. [PubMed: 2337607] b) Makhatadze GI, Loladze VV, Ermolenko DN, Chen X, Thomas ST. J. Mol. Biol. 2003; 327:1135–1148. [PubMed: 12662936]
32. Connelly PR, Aldape RA, Bruzzese FJ, Chambers SP, Fitzgibbon MJ, Fleming MA, Itoh S, Livingston DJ, Navia MA, Thomson JA, et al. Proc. Natl. Acad. Sci. U. S. A. 1994; 91:1964–1968. [PubMed: 7510408]
33. Clark AM, Labute P. J. Chem. Inf. Model. 2007; 47:1933–1944. [PubMed: 17715911]
34. Ryckmans T, Edwards MP, Horne VA, Correia AM, Owen DR, Thompson LR, Tran I, Tutt MF, Young T. Bioorg. Med. Chem. Lett. 2009; 19:4406–4409. [PubMed: 19500981]
35. Schrödinger Release 2017-3: QikProp. Schrödinger, LLC; New York, NY: 2017.
36. a) Di L, Kerns EH. Curr. Opin. Chem. Biol. 2003; 7:402–408. [PubMed: 12826129] b) Lipinski CA. Drug Discovery Today: Technol. 2004; 1:337–341.
37. Pajouhesh H, Lenz GR. NeuroRx. 2005; 2:541–553. [PubMed: 16489364]
38. Johnson TW, Dress KR, Edwards M. Bioorg. Med. Chem. Lett. 2009; 19:5560–5564. [PubMed: 19720530]
39. van Noord C, Eijgelsheim M, Stricker BH. Br. J. Clin. Pharmacol. 2010; 70:16–23. [PubMed: 20642543]
40. a) Rampersad SN. Sensors (Basel). 2012; 12:12347–12360. [PubMed: 23112716] b) Hamid R, Rotshteyn Y, Rabadi L, Parikh R, Bullock P. Toxicol. In Vitro. 2004; 18:703–710. [PubMed: 15251189]
41. a) Richon VM, Sandhoff TW, Rifkind RA, Marks PA. Proc. Natl. Acad. Sci. U. S. A. 2000; 97:10014–10019. [PubMed: 10954755] b) Klisovic MI, Maghraby EA, Parthun MR, Guimond M, Sklenar AR, Whitman SP, Chan KK, Murphy T, Anon J, Archer KJ, Rush LJ, Plass C, Grever MR, Byrd JC, Marcucci G. Leukemia. 2003; 17:350–358. [PubMed: 12592335] c) Bolden JE, Peart MJ, Johnstone RW. Nat. Rev. Drug Discovery. 2006; 5:769–784. [PubMed: 16955068] d) Neelarapu R, Holzle DL, Velaparthi S, Bai H, Brunsteiner M, Blond SY, Petukhov PA. J. Med. Chem. 2011; 54:4350–4364. [PubMed: 21548582] e) Sambucetti LC, Fischer DD, Zabludoff S, Kwon PO, Chamberlin H, Trogani N, Xu H, Cohen D. J. Biol. Chem. 1999; 274:34940–34947. [PubMed: 10574969]

42. a) Lutz L, Fitzner IC, Ahrens T, Geissler AL, Makowiec F, Hopt UT, Bogatyreva L, Hauschke D, Werner M, Lassmann S. Am. J. Cancer Res. 2016; 6:664–676. [PubMed: 27152243] b) Naldi M, Calonghi N, Masotti L, Parolin C, Valente S, Mai A, Andrisano V. Proteomics. 2009; 9:5437–5445. [PubMed: 19834889]

43. a) Kaufmann AM, Krise JP. J. Pharm. Sci. 2007; 96:729–746. [PubMed: 17117426] b) Zheng N, Tsai HN, Zhang X, Shedden K, Rosania GR. Mol Pharmaceutics. 2011; 8:1611–1618.

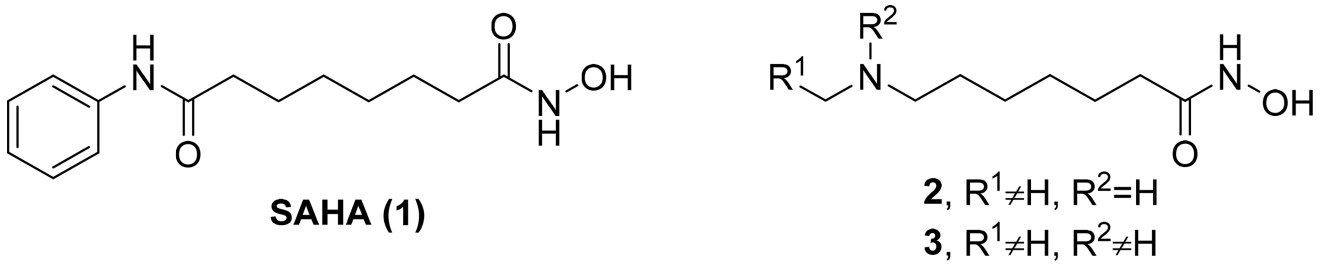

Figure 1.
The FDA-approved inhibitor SAHA (**1**) and general structure of amines **2** and **3**.

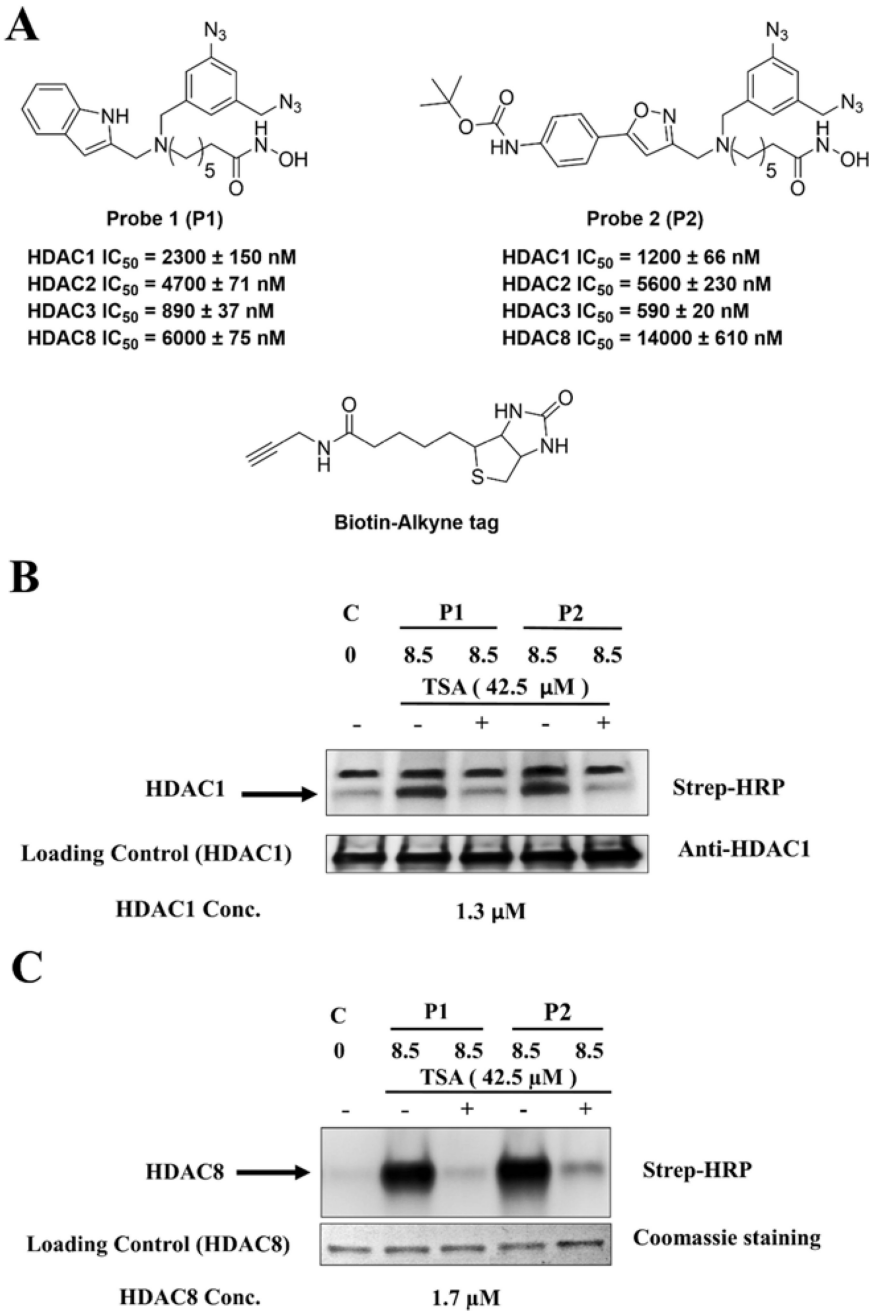

Figure 2. Photolabeling experiments against HDAC1 and HDAC8 using photolabeling probe 1 and 2

A) Chemical structures and activity profile of **P1**, and **P2**. B) HDAC1 (1.3 μM) was incubated with either photolabeling probes **P1** (8.5 μM) and **P2** or no probes control **C** in presence/absence of TSA (42.5 μM) for 2–3 h in the dark, followed by UV irradiation for 3 min to activate the aromatic azido group to form a covalent bond with nearby reactive amino acids side chains, then the click chemistry reaction was initiated between benzyl azido group and biotin-alkyne tag (50 μM). After 1 h, protein samples were analyzed via Western blots using streptavidin conjugated horse radish peroxidase (Strep-HRP). C) Similar to panel B using HDAC8 at a final concentration of 1.7 μM. IC_{50} values are expressed as mean ±

standard deviation of at least two independent experiments. The numbers are rounded to two significant figures. Equal loading of protein samples was validated using anti-HDAC1 antibody or coomassie staining.

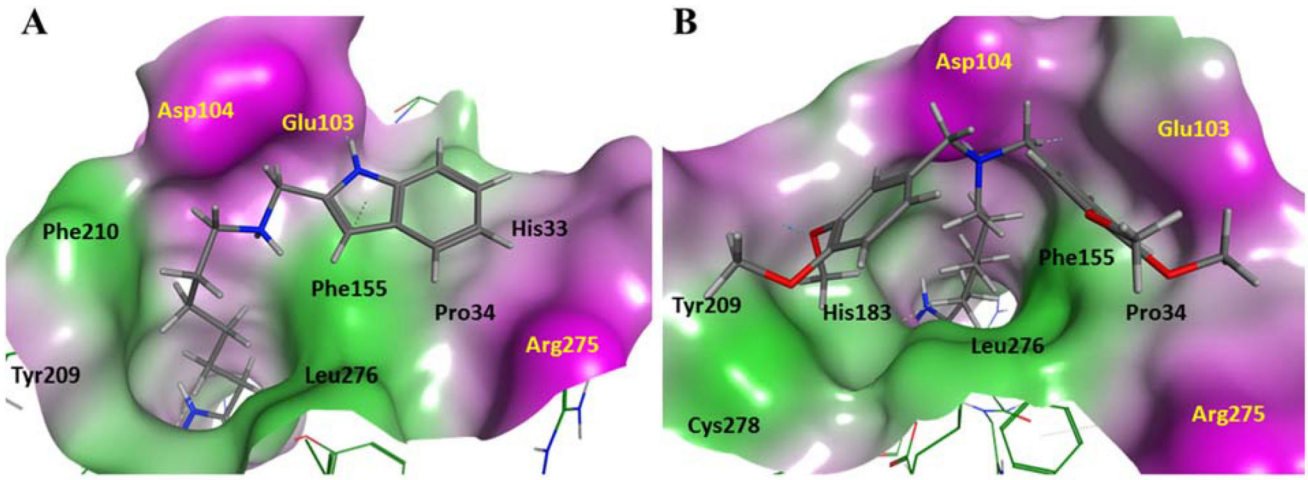

Figure 3.

(**A**) Docked pose of amine **2j** in the binding site of HDAC2 (PDB: 4LXZ) and (**B**) same for amine **3e**. The binding site surface is shown as a surface colored with lipophilic potential, green- lipophilic, purple – hydrophilic.

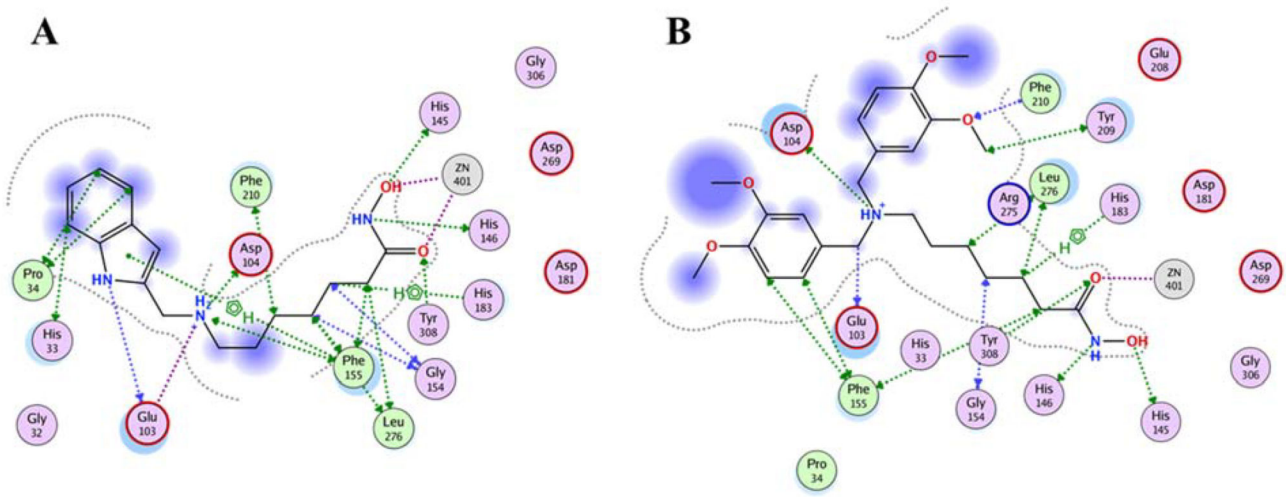

Figure 4.

Protein-ligand interaction between HDAC2 and (**A**) amine **2j** and (**B**) amine **2k** in PDB: 4LXZ. The 2D depiction of protein-ligand interactions in panels **A** and **B** is described in ref. [33]

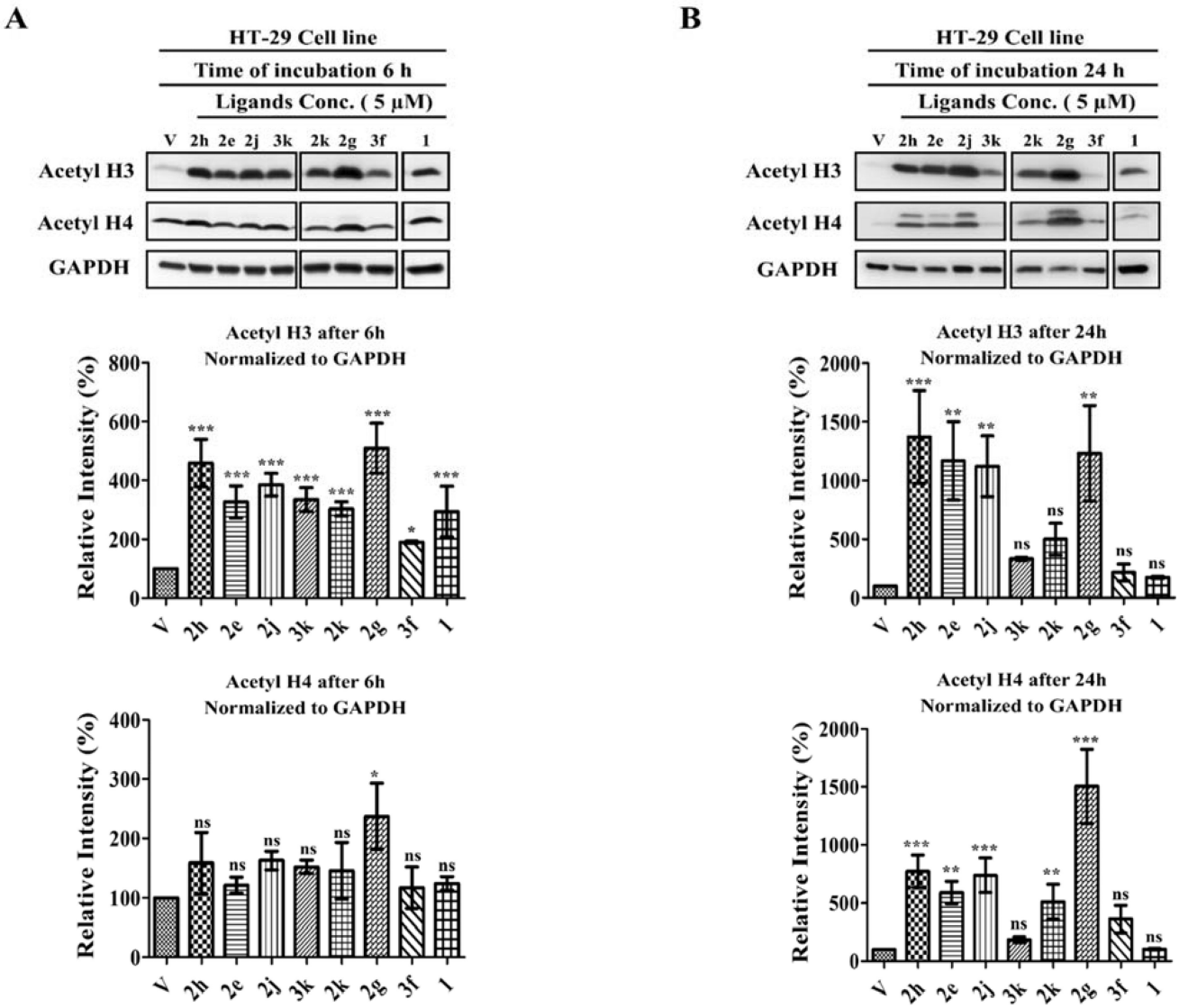

Figure 5. Analysis of histone H3 and H4 total acetylation status in HT-29 cells by Western blotting

HT-29 cells were treated with either DMSO (V), 5 μM of **1**, or 5 μM of **2e**, **2g**, **2h**, **2j**, **2k**, **3f**, or **3k** at A) 6 h and B) 24 h. One-way ANOVA revealed significant increase in acetylation of H3 and H4. The data is plotted as the average of at least 2 independent experiments +/− SD. (***, $p < 0.001$; **, $p < 0.01$; *, $p < 0.05$; ns, statistically nonsignificant).

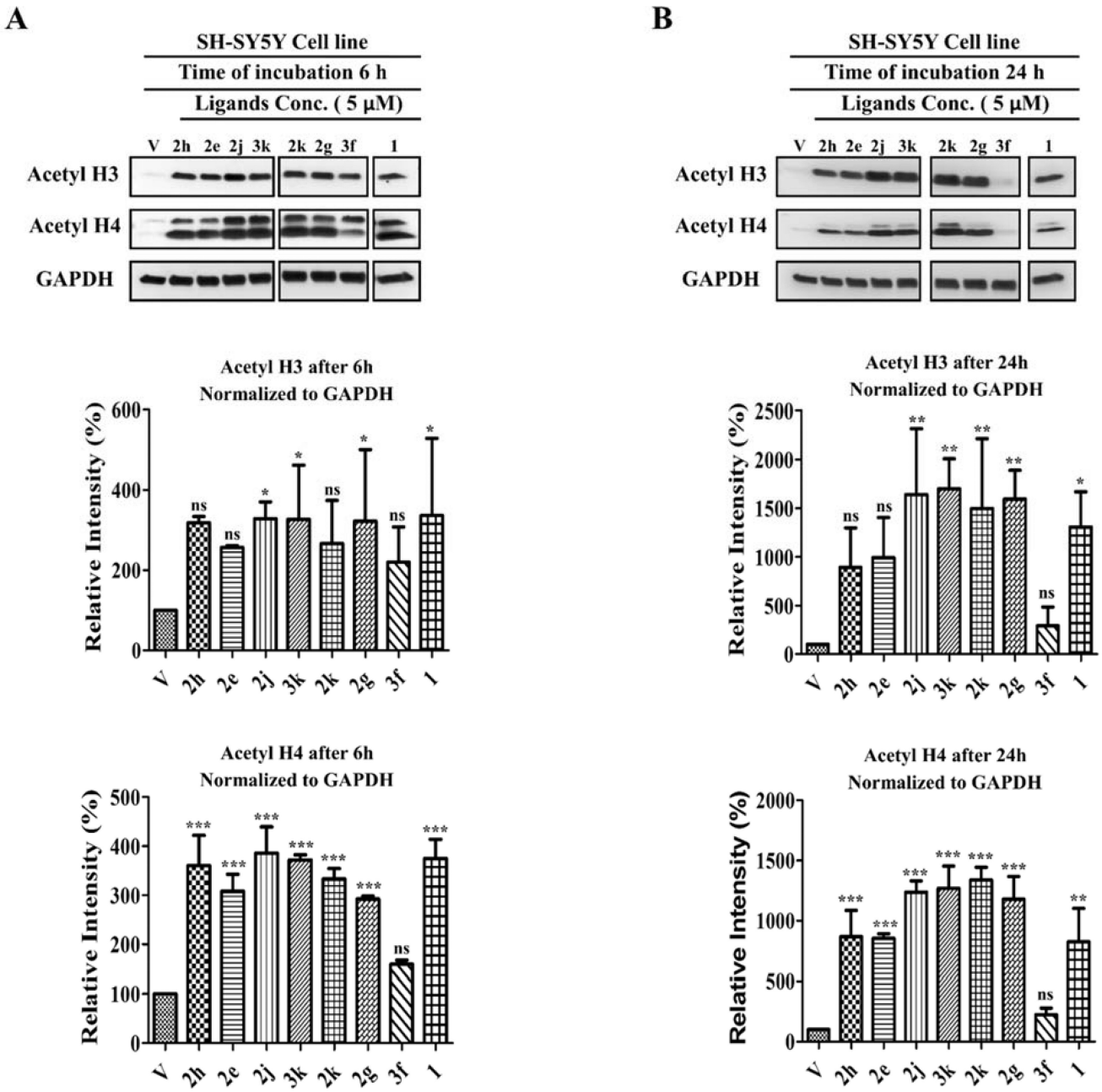

Figure 6. Analysis of histone H3 and H4 total acetylation status in SH-SH5Y by Western blotting

SH-SH5Y cells were treated with either DMSO (V), 5 μM of **1**, or 5 μM of **2e**, **2g**, **2h**, **2j**, **2k**, **3f**, or **3k** at A) 6 h and B) 24 h. One-way ANOVA revealed significant increase in acetylation of H3 and H4. The data is plotted as the average of at least 2 independent experiments +/− SD. (***, $p < 0.001$; **, $p < 0.01$; *, $p < 0.05$; ns, statistically nonsignificant).

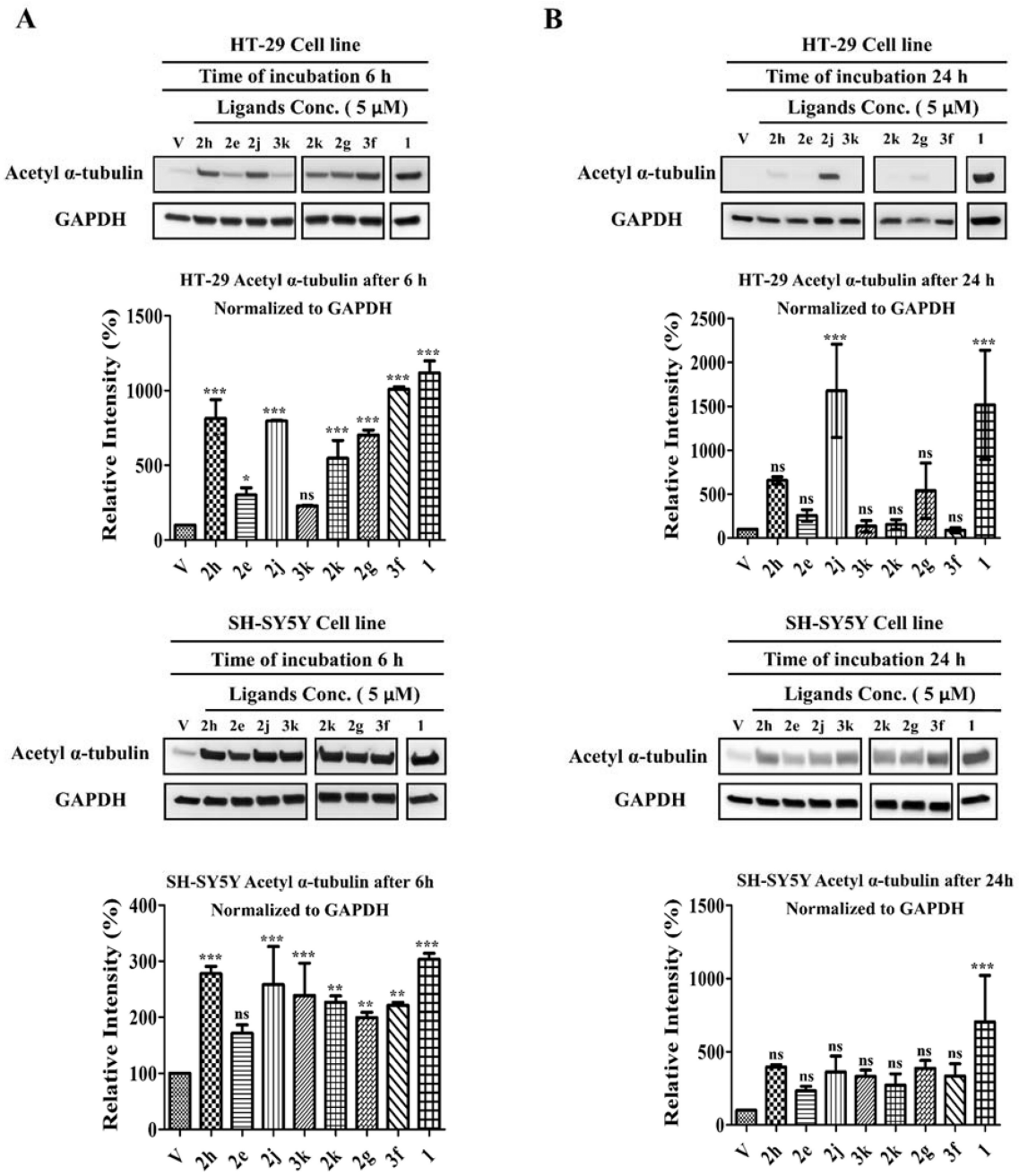

Figure 7. Analysis of tubulin total acetylation status in HT29 and SH-SH5Y by Western blotting

HT-29 and SH-SH5Y cells were treated with 5 μM of **1** and amine-based HDAC inhibitors **2e**, **2g**, **2h**, **2j**, **2k**, **3f**, and **3k** at A) 6 h and B) 24 h. One-way ANOVA revealed significant increase in acetylation of tubulin. The data is plotted as the average of at least 2 independent experiments +/− SD. (***, $p < 0.001$; **, $p < 0.01$; *, $p < 0.05$; ns, statistically nonsignificant).

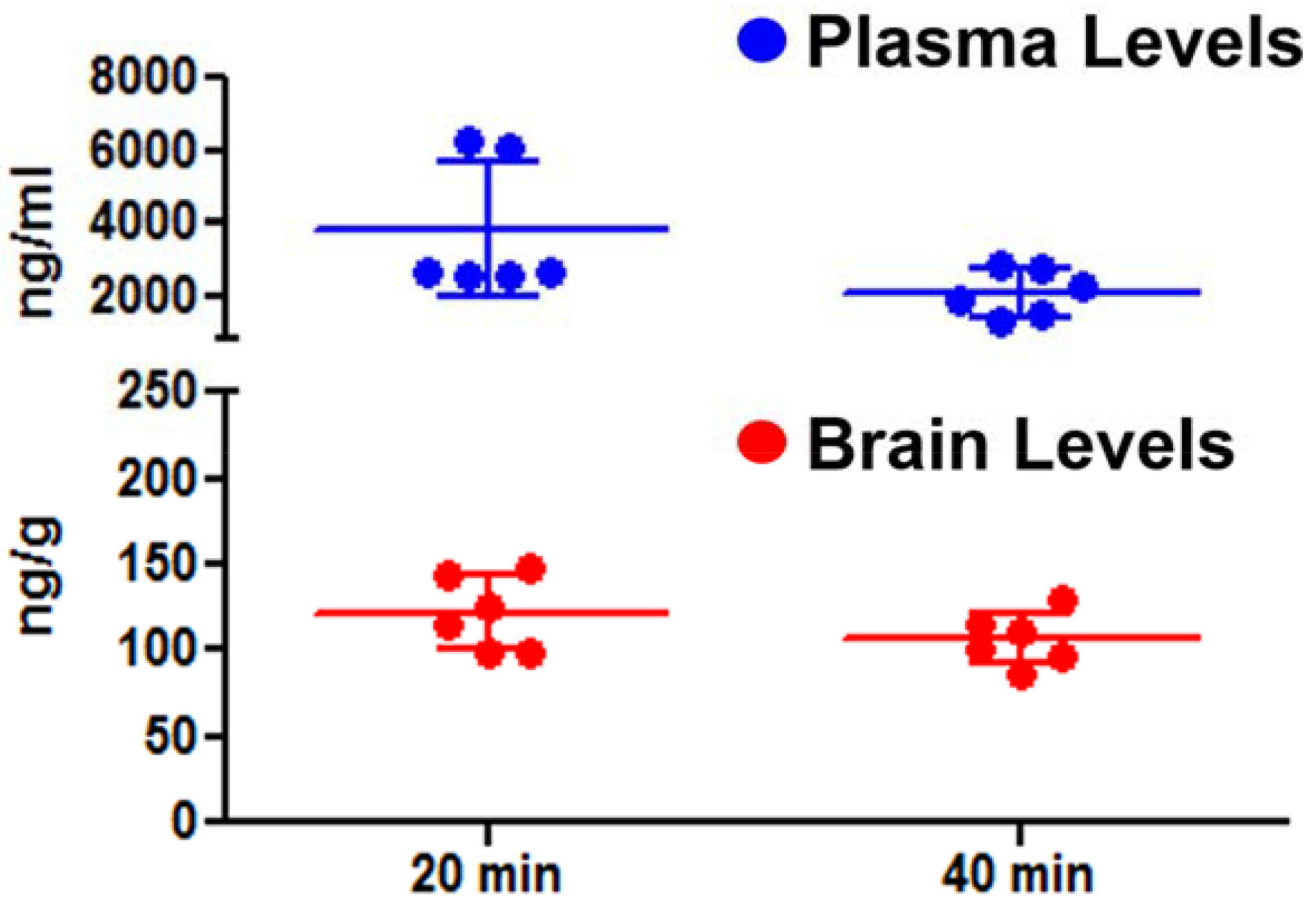

Figure 8. Plasma and brain concentrations of secondary amine-based HDAC inhibitor 2j

Spraugue Dawley rats were treated with the compound at the doses of 25 mg/kg via i.p. injection. Plasma and whole brains were collected at 20 and 40 min after dosing ($n = 3$ for each time point in all other treatments). Data are presented as mean ± SD and include 2 technical replicates for each sample.

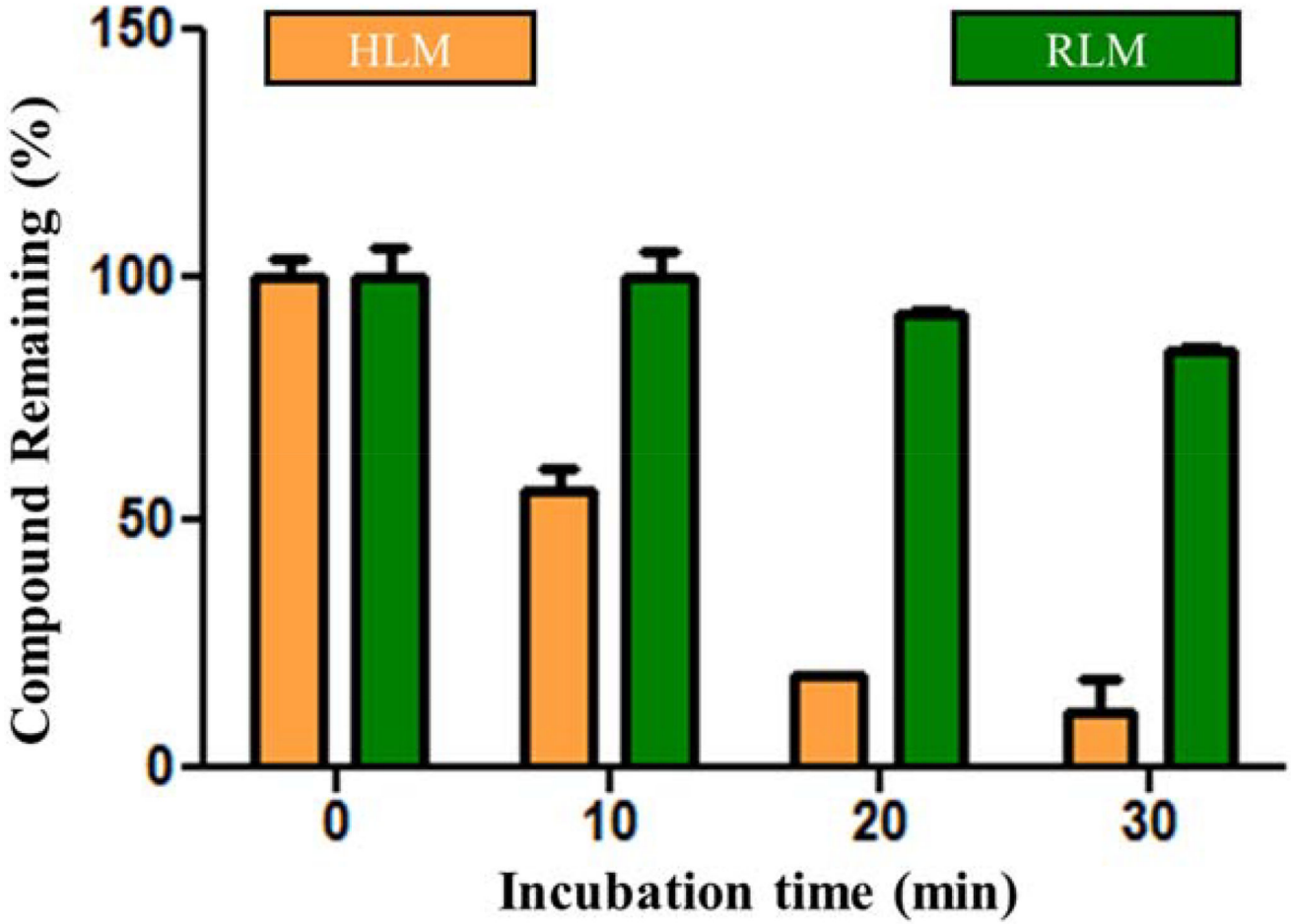

Figure 9. Analysis of microsomal stability of Secondary amine-based HDAC inhibitor 2j

Percentage of remaining secondary amine-based HDAC inhibitor **2j** after incubating with human liver microsomes (HLM, orange bars) and with rat liver microsomes (RLM, green bars). At each time point the remaining portion was determined by comparing with that from same incubations in the absence of NADPH (n = 3 for each time point). Data presented in mean ± SD.

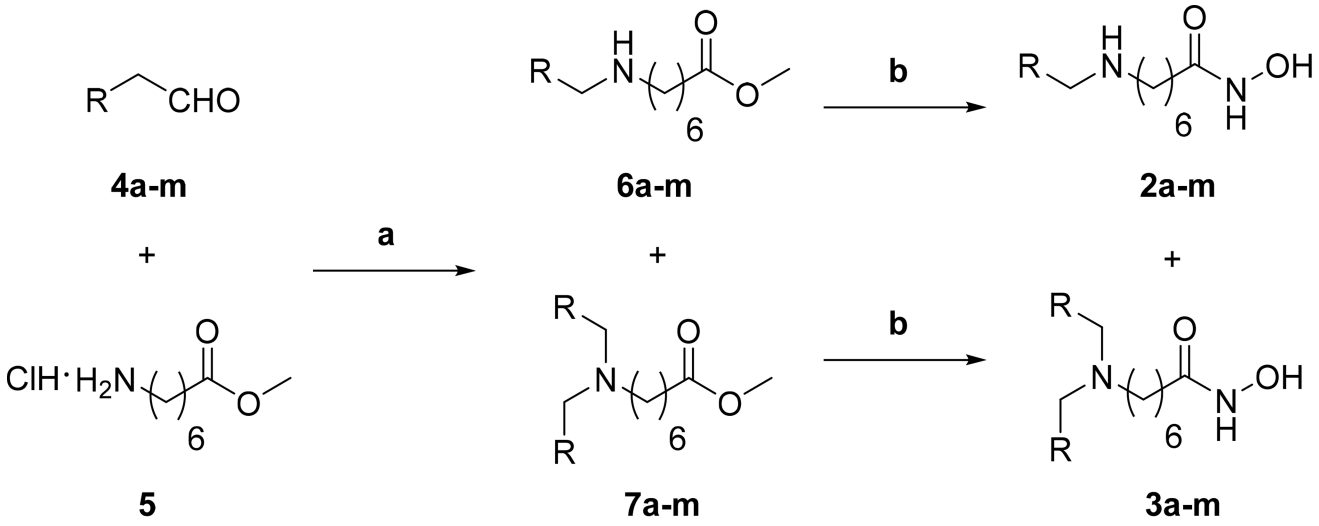

Reagents and conditions: (a) Et_3N (2.5 eq), STAB (2.5 eq), CH_2Cl_2, rt, 5 h, (yields: **6a-m** 50-60%, **7a-m** 15-30%); (b) $NH_2OH{\cdot}HCl$ (200 eq), KOH (205 eq), MeOH, 0 °C−rt, 3 h (yields: 40-80%).

Scheme 1.
General synthetic scheme for secondary and tertiary amine-based HDAC inhibitors.

ChemMedChem. Author manuscript; available in PMC 2018 December 19.

Table 1

Inhibition profile of secondary and tertiary amine-based HDAC inhibitors.

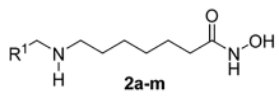

2a-m

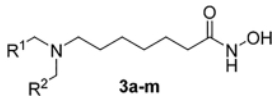

3a-m

Compd	R^1	R^2	IC_{50} (nM)[a]			
			HDAC1	HDAC2	HDAC3	HDAC8
1	-		22.0 ± 5.0	200 ± 14	21 ± 8.5	210 ± 15
2a		**H**	340 ± 3.5	3100 ± 790	430 ± 380	1800 ± 130
3a			1100 ± 59	2700 ± 670	1100 ± 120	4000 ± 370
2b	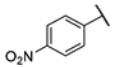	**H**	220 ± 25	2900 ± 60	1000 ± 200	2100 ± 50
3b	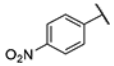	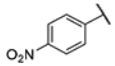	2000 ± 92	4000 ± 210	1400 ± 61	4900 ± 550
2c		**H**	220 ± 29	1500 ± 110	240 ± 10.0	1700 ± 120
3c			3900 ± 100	10000 ± 320	3600 ± 37	8300 ± 1100
2d	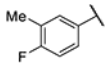	**H**	140 ± 12	790 ± 38	190 ± 34	2800 ± 100
3d	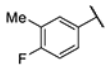	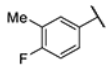	3400 ± 97	15000 ±1800	4700 ± 84	9800 ± 310

Compd	R^1	R^2	IC_{50} (nM)[a]			
			HDAC1	HDAC2	HDAC3	HDAC8
2e		H	210 ± 18	1800 ± 98	180 ± 5.0	1800 ± 76
3e			270 ± 11	1100 ± 560	290 ± 26	2100 ± 83
2f		H	430 ± 22	3200 ± 130	310 ± 13	1600 ± 380
3f			480 ± 65	4000 ± 370	480 ± 29	1400 ± 160
2g		H	39 ± 3.00	320 ± 13	68 ± 2.0	320 ± 26
3g			1100 ± 47	4200 ± 250	950 ± 49	5400 ± 470
2h		H	130 ± 10	840 ± 94	170 ± 9.0	270 ± 44
3h			500 ± 45	4200 ± 52	760 ± 26	4200 ± 580
2i		H	250 ± 19	1800 ± 140	120 ± 7.0	720 ± 20

Compd	R^1	R^2	IC_{50} (nM)[a]			
			HDAC1	HDAC2	HDAC3	HDAC8
3i			680 ± 66	3700 ± 160	2900 ± 240	2100 ± 80
2j[b]		H	61 ± 5.9	260 ± 15	25 ± 2.0	620 ± 42
3j			340 ± 20	3700 ± 98	1300 ± 160	4600 ± 100
2k		H	130 ± 20	620 ± 28	160 ± 12	800 ± 30
3k			1300 ± 160	3700 ± 98	440 ± 11	6400 ± 70
2l		H	48 ± 5.6	690 ± 31	38 ± 2.0	550 ± 94
3l			840 ± 35	3000 ± 75	1100 ± 123	4100 ± 30
2m		H	1500 ± 110	3000 ± 140	1500 ± 91	2500 ± 350

Compd	R^1	R^2	IC_{50} (nM)[a]			
			HDAC1	HDAC2	HDAC3	HDAC8
3m			1700 ± 70	6700 ± 1100	1600 ± 92	25000 ± 3700

[a] IC_{50} values are expressed as mean ± standard deviation of at least two independent experiments. The numbers are rounded to two significant figures.

[b] HDAC6 IC_{50} = 67 ± 0.23 nM

Table 2

Selectivity profile of secondary and tertiary amine-based HDAC inhibitors.

Compd	Selectivity[a]		
	HDAC2/HDAC1	HDAC3/HDAC1	HDAC8/HDAC1
2a	9.1	1.3	5.3
3a	2.5	1	3.6
2b	13	4.5	9.5
3b	2	0.7	2.5
2c	6.8	1.1	7.7
3c	2.6	0.92	2.1
2d	5.6	1.4	20
3d	4.4	1.4	2.9
2e	8.6	0.86	8.6
3e	4.1	1.1	7.8
2f	7.4	0.72	3.7
3f	8.3	1	2.9
2g	8.2	1.7	8.2
3g	3.8	0.86	4.9
2h	6.5	1.3	2.1
3h	8.4	1.5	8.4
2i	7.2	0.48	2.9
3i	5.4	4.3	3.1
2j	4.2	0.41	10
3j	11	3.8	14
2k	4.8	1.2	6.2
3k	2.8	0.34	4.9
2l	14	0.8	11
3l	3.6	1.3	4.9
2m	2	1	1.7
3m	3.9	0.94	15

[a]Selectivity ratios are calculated by dividing the HDAC1, 2, 3, and 8 IC_{50} of an amine-based inhibitor by HDAC1 IC_{50} of the same inhibitor. The numbers are rounded to two significant figures.

Table 3

Physicochemical properties of secondary and tertiary amine-based HDAC inhibitors.

	Physicochemical Properties[a]									
Compd	**Slog*P***	**log*S***	**TPSA**	**MW**	**log*D***	**log*hERG***	**LLE HD1**	**LLE HD2**	**LLE HD3**	**LLE HD8**
1	2.5	−2.9	78	260	1.9	−4.3	5.2	4.2	5.2	4.2
2a	2.5	−2.2	61	250	−0.73	−5.0	4.0	3.0	3.9	3.2
3a	4.7	−4.1	53	340	1.8	−5.2	1.3	0.89	1.3	0.72
2b	2.4	−3.0	110	300	−0.40	−4.9	4.3	3.1	3.6	3.3
3b	4.5	−5.7	140	430	2.4	−5.7	1.2	0.90	1.4	0.82
2c	2.6	−2.5	61	270	−0.51	−4.8	4.0	3.2	4.0	3.1
3c	5.0	−4.7	53	380	2.2	−5.5	0.45	0.044	0.49	0.13
2d	2.9	−2.7	61	280	−0.30	−4.8	3.9	3.2	3.8	2.6
3d	5.6	−5.0	53	410	2.6	−5.4	−0.10	−0.75	−0.25	−0.56
2e	2.5	−2.3	80	310	−0.82	−4.8	4.2	3.2	4.2	3.2
3e	4.7	−4.3	89	460	1.5	−5.6	1.9	1.2	1.8	0.97
2f	1.9	−0.95	74	250	−0.73	−4.7	4.5	3.6	4.6	3.9
3f	3.5	−1.6	78	340	1.2	−5.5	2.9	1.9	2.9	2.4
2g	3.7	−4.1	61	300	0.42	−5.6	3.8	2.8	3.5	2.8
3g	7.0	−7.9	53	440	4.0	−7.0	−1.0	−1.6	−0.96	−1.7
2h	2.2	−2.2	80	290	−1.3	−4.9	4.7	3.8	4.5	4.3
3h	4.1	−4.0	89	430	0.64	−5.8	2.2	1.2	2.0	1.2
2i	4.8	−4.4	76	410	2.2	−6.1	1.8	0.97	2.1	1.4
3i	9.2	−8.4	81	660	7.4	−7.2	−3.1	−3.8	−3.7	−3.7
2j	3.0	−2.7	77	290	0.087	−5.3	4.2	3.6	4.6	3.2
3j	5.6	−5.0	84	420	3.20	−6.6	0.83	−0.21	0.24	−0.30
2k	3.6	−3.3	74	330	0.31	−6.0	3.3	2.6	3.2	2.5
3k	6.8	−6.4	78	490	3.8	−7.9	−0.92	−1.4	−0.45	−1.6
2l	4.2	−4.4	61	330	1.7	−5.8	3.1	1.9	3.2	2.0
3l	8.1	−8.5	53	500	6.4	−7.7	−2.1	1.9	3.2	2.0
2m	4.5	−4.7	130	430	1.1	−6.3	1.3	1.0	1.3	1.1

Compd	Physicochemical Properties[a]									
	Slog*P*	log*S*	TPSA	MW	log*D*	log*hERG*	LLE HD1	LLE HD2	LLE HD3	LLE HD8
3m	8.7	−9.0	180	700	5.0	−7.9	−2.9	−3.5	−2.9	−4.1

[a]Physicochemical properties were calculated with MOE and QikProp/Schrödinger software. The numbers are rounded to two significant figures. Detailed description of these parameters can be found in the method section in supplementary information. LLE HD1, 2, 3, and 8 stands for lipophilic ligand efficiency calculated for HDAC1, HDAC2, HDAC3, and HDAC8, respectively.

Table 4

Cytotoxicity of **1** and amine-based HDAC inhibitors **2g**, **2h**, **2j–l**, **3e**, **3f** against HT-29, SH-SY5Y, and MCF-7 cell lines.

Compd	HT-29[a]		SH-SY5Y[a]		MCF-7[b]	
	24 h	48 h	24 h	48 h	24 h	48 h
1	> 50	1.0 ± 0.11	> 50	1.5 -± 0.1	48%	68%
2g	> 50	1.1 ± 0.11	> 50	1.2 ± 0.22	19%	46%
2h	> 50	2.2 ± 0.68	> 50	2.4 ± 0.32	24%	56%
2j	> 50	2.1 ± 0.17	> 50	1.3 ± 0.39	61%	71%
2k	35 ± 4.0	2.3 ± 0.21	13 ± 1.6	1.5 ± 0.12	66%	63%
2l	24 ± 1.4	2.5 ± 0.65	15 ± 1.1	6.1 ± 0.78	63%	71%
3e	> 50	4.2 ± 0.37	> 50	3.5 ± 0.16	55%	60%
3f	> 50	48 ± 1.4	> 50	23 ± 1.8	NA[c]	8.7%

[a] EC_{50} values (μM) are expressed as mean ± standard deviation of four independent experiments (n=4).

[b] Growth inhibition percentage at 10 μM.

[c] NA = no inhibition at 10 μM.